MR evaluation of brain iron in children with cerebral infarction.

P A Cross, S W Atlas and R I Grossman

AJNR Am J Neuroradiol 1990, 11 (2) 341-348
http://www.ajnr.org/content/11/2/341

MR Evaluation of Brain Iron in Children with Cerebral Infarction

Patricia A. Cross[1]
Scott W. Atlas
Robert I. Grossman

Young children and infants normally have essentially no detectable brain iron. We evaluated brain iron patterns on 23 MR scans in 20 patients under 6 years of age with clinical and MR-documented cerebral infarctions in an attempt to further understand the neuropathologic phenomenon of increased iron deposition, which has been observed in other disease states. MR was performed at 1.5 T with spin-echo sequences from 1 day to 4 years after infarction. MR scans were interpreted without knowledge of clinical information and were assessed for (1) location and character (i.e., bland or hemorrhagic) of infarct, and (2) nonheme iron (i.e., marked hypointensity on long TR/TE images) in the basal ganglia, red nuclei, substantia nigra, thalami, dentate nuclei, and deep white matter. Sixteen of 20 infarctions were associated with increased iron. Six of seven cases with unilateral iron deposition had ipsilateral infarctions. The location (deep versus cortical) and age of the infarction had no apparent bearing on iron patterns.

We conclude that increased brain iron is commonly associated with cerebral infarction and is nonspecific, rather than a marker of movement disorders. Since iron may arise from either interruption of transport pathways or directly from cell injury and, in fact, iron itself may propagate the tissue injury, this finding may have important clinical and pathophysiologic implications in ischemic brain injury.

***AJNR* 11:341–348, March/April 1990**

Recently, much attention has been given to the MR imaging appearance of normal, as well as pathologic, iron deposition in the brain. It has been well documented in necropsy studies and more recently confirmed on in vivo MR imaging that iron normally accumulates at specific intracerebral sites in a progressive fashion that is related to age [1–4] (Figs. 1 and 2). Furthermore, abnormal levels of iron in the basal ganglia and thalami have been documented, both pathologically and with MR imaging, in many degenerative disorders of the central nervous system [5–12].

The presence of abnormal iron is often easier to recognize in the brain of infants and children than in the adult brain, since the young child has essentially no iron in the deep gray matter nuclei [2, 4] (Fig. 1). Prominent iron content in the basal ganglia, thalami, and deep white matter was recently reported in four young children suffering diffuse ischemic-anoxic brain injury [13]. In this study, we evaluated the intracerebral iron pattern on MR images in 20 patients under 6 years of age who had MR-documented cerebral infarctions.

Subjects and Methods

Between January 1984 and June 1988, 30 patients under the age of 6 years with clinical symptoms and signs consistent with cerebral infarction were referred for MR evaluation of the brain. Twenty of these had MR evidence of infarction. These 20 consisted of 11 males and nine females, ranging in age from 3 days to 5 years, 8 months. MR was performed from 1 day to 4 years after onset of symptoms. Presenting complaints, pertinent history, and/or

Received May 11, 1989; revision requested June 19, 1989; revision received August 2, 1989; accepted August 3, 1989.

Presented at the annual meeting of the American Society of Neuroradiology, Orlando, March 1989.

[1] All authors: Department of Radiology, Hospital of the University of Pennsylvania, 3400 Spruce St., Philadelphia, PA 19104. Address reprint requests to S. W. Atlas.

0195–6108/90/1102–0341

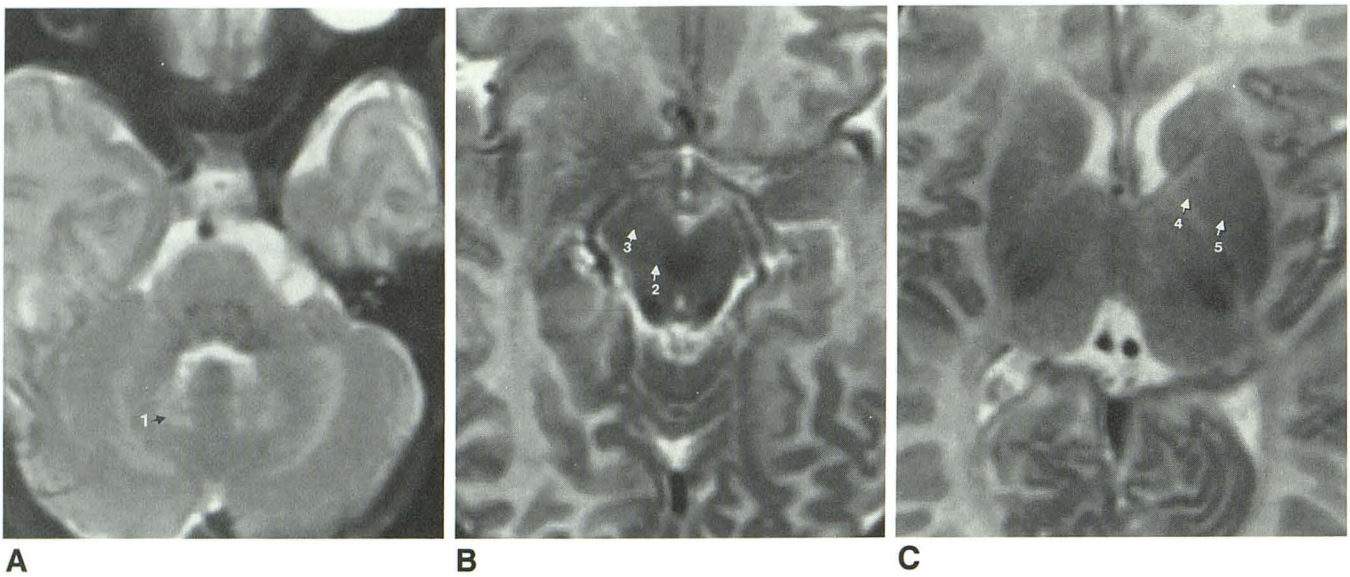

Fig. 1.—*A–C*, Normal MR brain iron pattern in 2-week-old infant (axial MR, 3000/120, inferior to superior). Note absence of significant hypointensity in deep gray matter structures (1 = dentate nucleus, 2 = red nucleus, 3 = substantia nigra, 4 = globus pallidus, 5 = putamen) in these serial long TR/long TE MR images, correlating to pathologically documented absence of stainable iron in the neonatal brain. Central hypointensity medial to red nuclei in *B* relates to decussation of superior cerebellar peduncles.

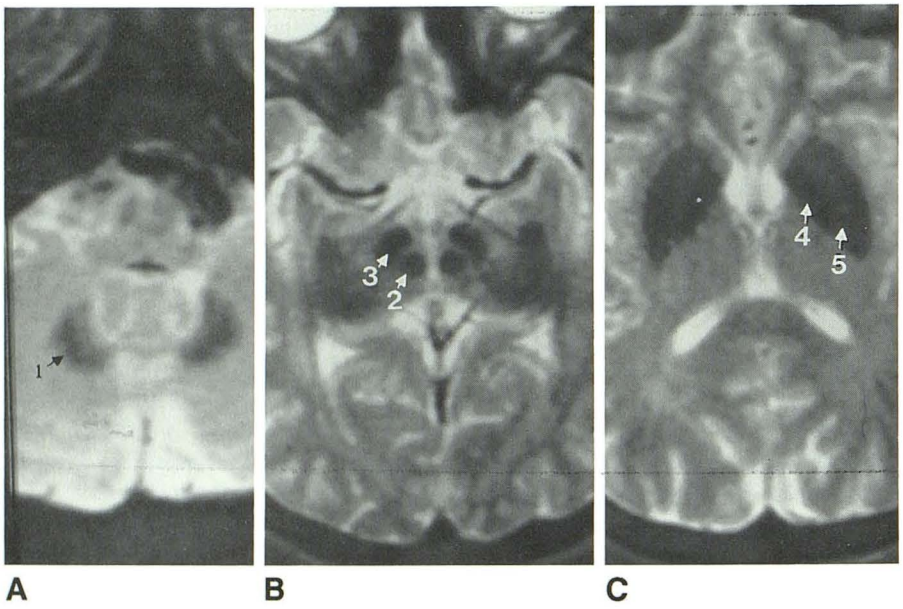

Fig. 2.—*A–C*, Normal MR brain iron pattern in 80-year-old (axial MR, 3000/90, inferior to superior). In distinction to the absence of detectable iron seen in neonates (Fig. 1), the senescent brain shown here demonstrates significant iron deposition in deep gray matter structures (1 = dentate nucleus, 2 = red nucleus, 3 = substantia nigra, 4 = globus pallidus, 5 = putamen), seen as marked hypointensity in this clinically normal elderly adult.

predisposing factors to cerebral infarction in these 20 patients included hemiparesis (nine), seizures (seven), neonatal asphyxia (five), cranial nerve palsies (three), otitis media (two), meningitis (two), upper respiratory infection (two), head trauma (two), lethargy (one), intracranial neoplasm (one), hemolytic-uremic syndrome (one), idiopathic thrombocytopenic purpura (one), and Chediak-Higashi syndrome (one).

All MR imaging was performed with spin-echo techniques at 1.5 T (General Electric, Milwaukee). Long repetition time (TR), 2000–3000, images were obtained in all cases. Multiple echo delays (two to four) were acquired by using short echo times (TE) of 20–30 and long TEs of 80–90. Interecho times ranged from 20–60. In all cases, short TR (600/20, 25) images were also obtained. Twenty-three scans of 20 patients were reviewed (three patients has serial MR scans, which were obtained 5, 12, and 15 months, respectively, after the initial scan). MR scans were interpreted with the reader blinded to any localizing clinical history.

MR images were reviewed specifically for the presence and location of the infarction, as well as for the presence of hemorrhage within the region of abnormality. Additionally, the long TR images were reviewed for evidence of hypointensity consistent with non–heme-associated iron at the following locations: dentate nucleus, red nucleus, substantia nigra, globus pallidus, putamen, caudate nucleus, thalamus, and deep white matter. (Note: the presence of iron was indicated by hypointensity relative to gray matter, which was solely evident and/or became more prominent on the long TR/longTE scan and was not associated with any mass effect.) Any heme-associated iron that occurred within any of the aforementioned deep gray or

white matter structures precluded the evaluation of those structures for non–heme-associated iron, and therefore these regions were not included in the tabulation of iron accumulation (see Table 1).

Results

MR evidence of infarction was identified in all 20 patients included in the study. Fourteen of the 20 infarctions were unilateral. In six cases, the infarction was isolated to the cortex (five of six unilateral, one of six bilateral). Six of 20 involved the cortex and basal ganglia/thalami (four of six unilateral, two of six bilateral), while eight of 20 were limited to the deep gray matter nuclei (five of eight unilateral, three of eight bilateral). Thirteen infarctions were bland, while seven demonstrated hemorrhage by MR criteria [14, 15]. In two of the seven hemorrhagic infarctions, heme-associated iron within basal ganglionic structures preempted evaluation of these areas for nonheme iron deposition.

Areas of selective or more profound hypointensity on long TR/TE images, consistent with nonheme iron, were seen in one or more deep gray matter nuclei or deep white matter in 16 of 20 cases. No cases demonstrated calcification on CT scans in the areas of MR-documented hypointensity. In the four cases without iron deposition, one had a hemorrhagic infarction involving the globus pallidus that precluded evaluation for nonheme iron in that structure. The frequency with which iron was found in these structures is summarized in Table 1. The red nucleus was involved most frequently (10 cases), followed by the substantia nigra (eight), thalamus (six), globus pallidus (five), putamen (four), caudate nucleus (three), and dentate nucleus (one). The deep white matter demonstrated iron deposition in four cases (Fig. 3). (Note that areas of hemorrhagic infarction were excluded from this tabulation, since we are concerned with nonheme iron only.)

Unilateral hypointensity in the basal ganglia or deep white matter on long TR/TE images was found in seven cases, six of which had unilateral infarction. In all six of these, the (predominant) iron was on the same side as the infarction (Figs. 3–6). Of these unilateral infarctions with unilateral iron, three were cortical infarctions (all bland by MR), and three involved the deep gray matter (two of three were hemorrhagic).

Examination of the results by clinical age of the infarction revealed that abnormal iron deposition was present regardless of the age of the infarction. Iron was found as early as 1 day and as late as 4 years from the time of the infarction. In one of the patients in whom serial MR scans were obtained, only the 12-month follow-up MR demonstrated iron deposition in the ipsilateral globus pallidus (Fig. 5). In the other two patients with serial MR scans (5 months and 15 months from their original scans, respectively), no change in the pattern of iron on MR images was found (Fig. 6).

There was no difference in the pattern of localization of nonheme iron between those infarctions that involved only basal ganglionic structures and those that were cortical in nature (see Table 1). The relationship between the age of the patient at the time of infarction and the pattern of brain iron on MR images was examined (see Table 1). Of the eight patients under the age of 6 months, five had abnormal iron, and all of these had bilateral iron.

MR evidence of hemorrhage at the site of infarction was found in seven of 20 cases. Six of these seven patients were scanned 1 month or less after the infarction, while one was scanned 3 months after the insult. Of the hemorrhagic infarctions, two were cortical (one of these was unilateral), one involved both cortex and ganglionic regions (unilateral), and four were limited to the basal ganglia/thalami (two of these were unilateral). Five of these seven cases showed iron in the infarcted ganglia and/or thalami on MR. However, nonheme iron was also noted at apparently noninfarcted nuclei (i.e., on the contralateral side) in three of these cases.

Discussion

Histochemical evidence that iron accumulates preferentially in the basal ganglia and thalami with normal aging as well as in association with a variety of neurodegenerative states has been documented [1–13, 16, 17]. The concentration of nonheme iron increases with age, as demonstrated by autopsy studies showing that there is essentially no stainable ferric iron in the newborn brain (by Perl's and Prussian blue methods) and there is a subsequent progressive accumulation throughout childhood and early adult development. The positive correlation of marked hypointensity on long TR/TE MR images with histochemical nonheme iron in the deep gray matter structures has been documented by Drayer et al. [18] and Rutledge et al. [7].

Hallgren and Sourander [2] found that ferric species accumulated rapidly in ganglionic sites with the greatest rate of physiologic deposition occurring before the age of 20 years. This temporal progression of accumulated brain iron with increases in age was recently confirmed by Aoki [4] on in vivo MR imaging (Figs. 1 and 2). Specifically, Aoki demonstrated that, just as in previous necropsy histochemical studies [2], iron on MR images was first seen in the globus pallidus, followed by the substantia nigra and red nucleus, and then lastly (and to a more variable degree) the dentate nucleus. According to Aoki, virtually no patients under the age of 10 years have marked hypointensity in the globus pallidus, red nucleus, substantia nigra, or dentate on long TR/TE MR images at 1.5 T (Fig. 1). By inference from the MR data of Aoki [4] and autopsy data of Hallgren and Sourander [2], this corresponds to levels of iron less than approximately 10–15 mg/100 g brain tissue, which seems to be the threshold for the detection of ferric iron when using conventional MR techniques and parameters. It should be noted that many operator-dependent technical factors influence the appearance of iron on MR images, including the magnitude of the applied magnetic field, the mode of signal acquisition (i.e., whether a radiofrequency pulse is used to refocus spins, as in a spin-echo sequence, or if gradient reversal is utilized for signal acquisition), the specific TR, TE, and interecho interval (i.e., the time between consecutive 180° refocusing pulses for a given TR) [19]. For the purposes of this study, we used a 1.5-T system with a TR and TE within the range commonly used for long TR/TE images and a conventional interecho

TABLE 1: Patient Data

Patient No.	Age (months)	Infarct Location (side)	Infarct Location (cortical vs ganglionic)	? Hemorrhage	Age of Infarct (months)	D (right)	D (left)	SN (right)	SN (left)	RN (right)
1	7	Left	Cortical	No	0.03	0	0	0	0	0
2*	48	Bilateral	Cortical	No	0.3	0	0	+	+	+
2	60	Bilateral	Cortical	No	16	0	0	+	+	+
3	1	Right	Cortical	Yes	1	0	0	0	0	0
4	36	Left	Cortical	No	12	0	0	0	0	0
5	14	Left	Cortical	No	14	0	0	+	+	+
6	18	Right	Cortical	No	3	0	0	+	+	+
7	54	Left	Cortical and ganglionic	No	0.03	0	0	0	0	0
8	0.25	Bilateral	Cortical and ganglionic	Yes	0.25	0	0	0	0	0
9	0.5	Left	Cortical and ganglionic	Yes	0.5	0	0	0	0	0
10	4	Right	Cortical and ganglionic	No	0.5	0	0	+	+	+
11	1	Bilateral	Cortical and ganglionic	No	1	0	0	+	+	+
12	60	Left	Cortical and ganglionic	No	48	0	0	0	0	+
13	0.1	Bilateral	Ganglionic	Yes	0.1	0	0	0	0	0
14	0.25	Bilateral	Ganglionic	Yes	0.25	0	0	0	0	0
15*	67	Left	Ganglionic	No	0.75	0	0	+	+	+
15	79	Left	Ganglionic	No	13	0	0	+	+	+
16	36	Left	Ganglionic	No	1	+	+	+	+	+
17*	19	Left	Ganglionic	No	1.5	0	0	0	0	0
17	24	Left	Ganglionic	No	6.5	0	0	0	0	0
18	4	Bilateral	Ganglionic	Yes	3	0	0	0	0	+
19	45	Bilateral	Ganglionic	No	12	0	0	0	0	0
20	68	Right	Ganglionic	Yes	1	0	0	0	0	1

* These patients each had two separate MR scans.

Note.—0 = isointense with normal gray matter, + = hypointense and consistent with iron deposition, D = dentate, SN = substantia nigra, RN = red nucleus, GP = globus pallidus, P = putamen, C = caudate, T = thalamus, DWM = deep white matter.

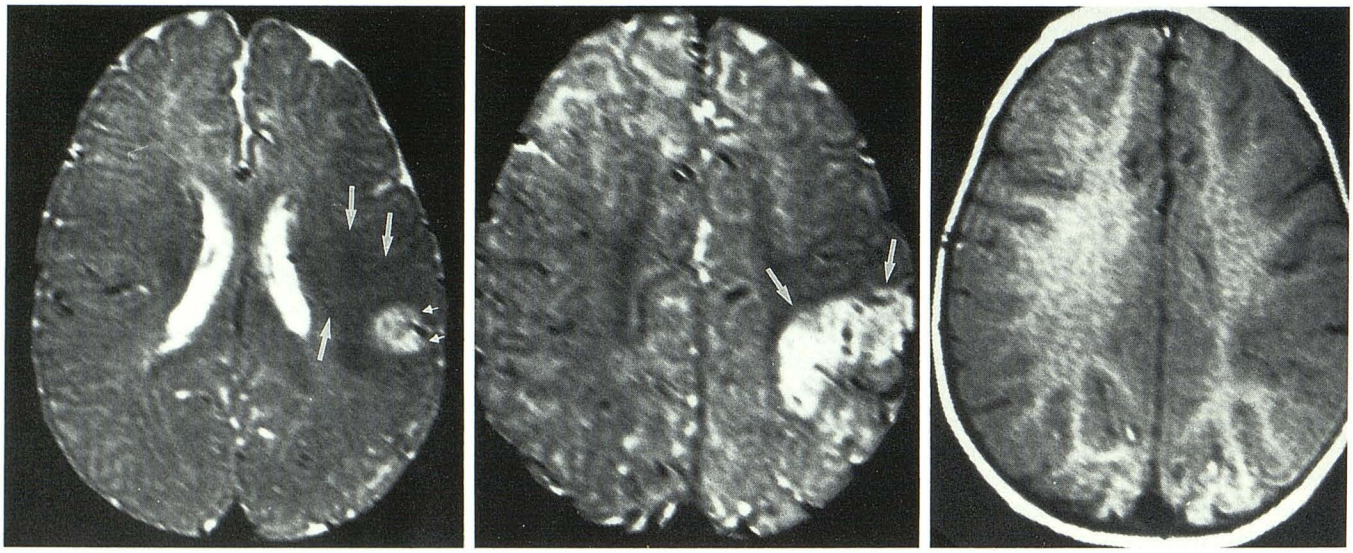

Fig. 3.—*A–C*, 1-day-old left parietal infarct with extensive white matter iron deposition in 7-month-old patient (axial MR, 2500/80 [*A* and *B*], 600/20 [*C*]). Note diffuse white matter hypointensity (*large arrows* in *A*) in long TR/TE images (*A* and *B*) consistent with iron deposition in white matter adjacent to focal hyperintense left parietal lobe infarct (*small arrows* in *A*). There is no evidence of abnormal hyperintensity on the short TR/TE image (*C*).

interval for most neuroradiologic multiecho MR imaging schemes.

In our study we limited the patient population to those under 6 years old; that is, to an age group in which virtually no iron has been found in the brain by either histologic study or MR examination [2, 4]. Therefore, the MR demonstration of *any* deep gray or white matter iron in our patients was considered abnormal and presumed to be related to the patient's known infarction. Furthermore, in six of seven patient with unilateral brain iron, the iron was on the side of the infarction, implicating the infarction as the reason for the presence of iron.

RN (left)	GP (right)	GP (left)	P (right)	P (left)	C (right)	C (left)	T (right)	T (left)	DWM (right)	DWM (left)
0	0	0	0	0	0	0	0	0	0	+
+	0	0	0	0	0	0	0	0	0	0
+	0	0	0	0	0	0	0	0	0	0
0	0	0	0	0	0	0	0	0	0	0
0	0	0	0	+	0	+	0	+	0	+
+	0	0	0	0	0	0	+	+	0	0
+	+	+	+	+	0	0	+	+	0	0
0	0	+	0	0	0	0	0	0	0	0
0	+	+	0	0	0	0	0	0	0	0
0	0	0	0	0	0	0	0	0	0	0
+	0	0	0	0	0	0	0	0	+	0
+	+	+	+	+	+	+	0	0	+	+
+	0	0	0	0	0	0	0	0	0	0
0	Heme	Heme	0	0	0	0	0	0	0	0
0	Heme	Heme	0	0	+	+	Heme	Heme	0	0
+	0	0	0	0	0	0	0	0	0	0
+	0	+	0	0	0	0	0	0	0	0
+	0	0	0	0	0	0	0	0	0	0
0	0	0	0	0	0	0	0	+	0	0
0	0	0	0	0	0	0	+	0	0	0
+	0	0	+	0	0	0	0	+	0	0
0	0	0	0	0	0	0	0	0	0	0
1	1	0	0	0	0	0	0	0	0	0

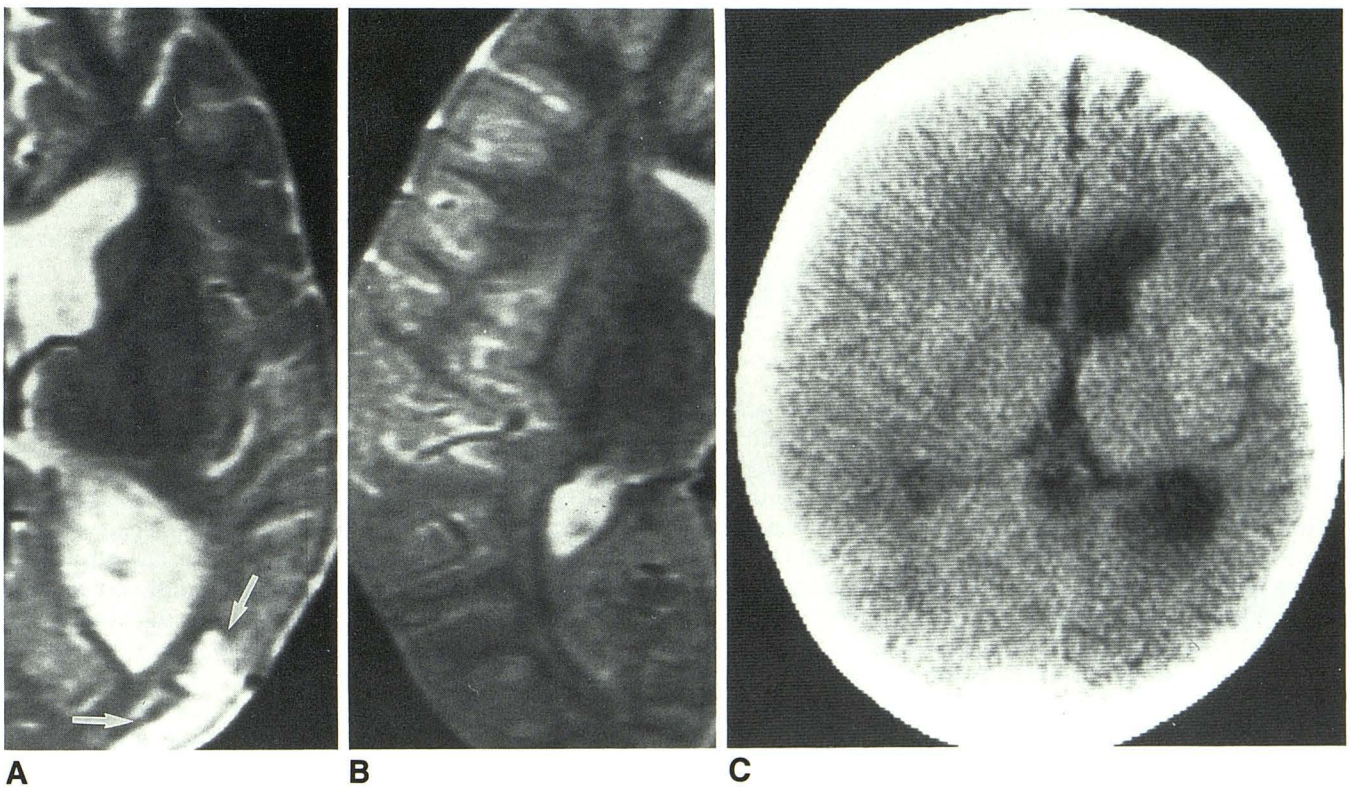

Fig. 4.—*A–C*, Basal ganglionic iron deposition 1 year after left parietooccipital cortical infarct in 3-year-old patient at time of scan. Axial MR, 2500/80, ipsilateral to infarct (*A*); axial MR, 2500/80, on contralateral normal side (*B*); axial CT (*C*). Diffuse hypointensity in left caudate, putamen, and thalamus on side of 1-year-old parietooccipital infarct (*arrows* in *A*) indicates iron deposition. Compare hypointense signal intensity of involved basal ganglia on left side (*A*) to normal, higher intensity of basal ganglia of normal right side (*B*) (patient was rotated at time of scanning, so slices were selected to display same anatomic levels). Note that the MR-documented left ganglionic hypointensity is *not* due to calcification (*C*).

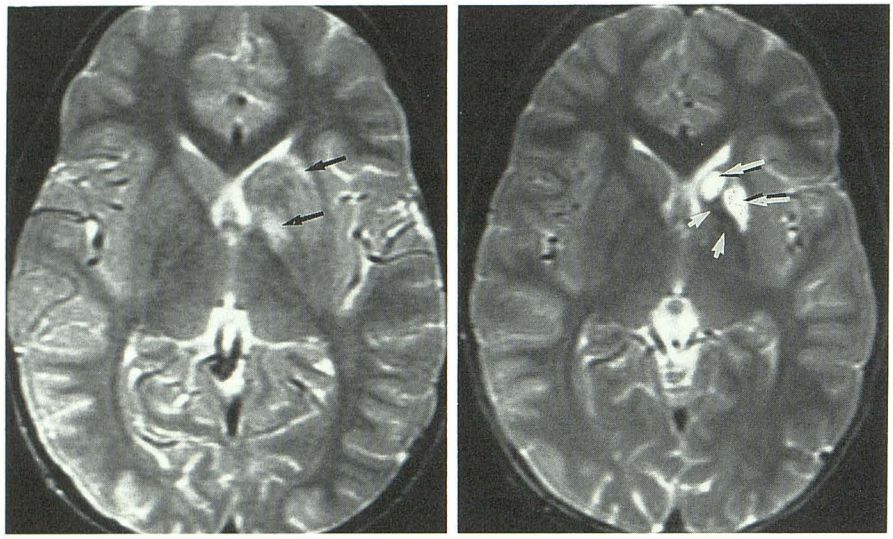

Fig. 5.—*A* and *B*, Delayed appearance of iron after left ganglionic bland infarction in 5½-year-old patient at time of initial scan (axial MR, 3000/90, 3 weeks [*A*] and 1 year [*B*] after infarction). Initial MR scan obtained 3 weeks after onset of symptoms (*A*) demonstrates high intensity in left basal ganglia (*arrows*), indicating region of nonhemorrhagic infarction, with no definite iron deposition. One year later, MR scan (*B*) demonstrates marked hypointensity indicating iron deposition in left globus pallidus and internal capsule (*short arrows*), adjacent to chronic infarct (*long arrows*).

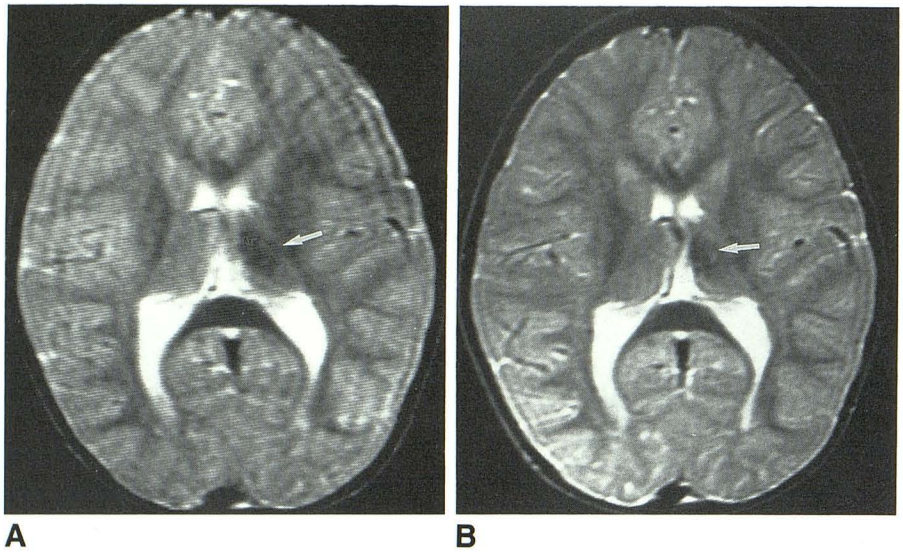

Fig. 6.—*A* and *B*, Persistence of thalamic iron deposition in 1½-year-old patient at time of initial scan (axial MR, 3000/90, 1½ months [*A*] and 6½ months [*B*] after infarction). Hypointense iron deposition in left thalamus (*arrows*), which was demonstrated on initial scan 1½ months after clinical infarction, persisted on follow-up scan 5 months later (a total of 6½ months after infarction).

Pathologic deposition of nonheme iron in the basal ganglia and thalami has been demonstrated histochemically and with MR imaging in association with several neurologic disorders [5–12], including lacunar infarction and after severe diffuse anoxic/ischemic injury [13, 20], and has been deemed particularly important in the imaging evaluation of movement disorders [6, 7]. Although nonheme iron is known to accumulate in the brain in many pathologic states, the mechanisms by which this occurs is not well understood. Studies of transferrin receptor densities by Hill et al. [21] and Jeffries et al. [22] suggest that iron bound to transferrin is taken up by capillary endothelial cells in the ganglionic and thalamic nuclei and then transported axonally to projection sites where it is used in local metabolism. In fact, iron is involved in many ways in brain metabolism [23]. Various iron enzymes are intimately involved in oxidative reactions and neurotransmitter metabolism. Iron plays a role in serotonin binding, dopamine receptor function, and in many monoamine synthetic and degradative enzymes. There is a significant overlap in the distributions of iron and gamma-aminobutyric acid (GABA) [24], probably indicating the involvement of iron in the metabolism of GABA.

It is possible that interruption of axonal projections by any cause, such as infarction, demyelination, or any other process, could result in abnormal accumulation of iron proximal to the insult (i.e., in the basal ganglia), since the iron could presumably still be taken up but not be transported via the pathologic axons. Such a mechanism of indirect iron accumulation is supported by our findings of high iron content in the deep gray matter structures months to years after infarction (Fig. 6) and also by our finding of unilateral deposition of iron on the same side as the infarction. Interestingly, there was no specific localization pattern of the site(s) of iron accumulation with reference to the presence of cortical versus deep infarction; that is, interruption of efferent or afferent

axonal pathways could not be differentiated by examining brain iron topography.

An additional mechanism for increased iron deposition in the ganglionic structures after ischemic brain injury has been postulated by some investigators and involves direct tissue injury [25–27]. After ischemic-anoxic injury, there is initially a loss of calcium ion homeostasis, followed by a loss of control of the intracellular iron pool during reperfusion. Iron, in its normal storage form as ferritin, is changed to low molecular weight species which, as a transition metal catalyst, can initiate free radical-mediated lipid peroxidation reactions resulting in brain tissue injury. Komara et al. [27] demonstrated statistically significant elevations in levels of both low-molecular-weight iron species and lipid peroxidation degradation products after cardiac arrest and resuscitation.

Administration of deferoxamine (an iron chelator) at the time of resuscitation reduced the concentration of these degradation products to levels statistically indistinguishable from nonischemic controls, implying a potential therapeutic role for iron chelators in preventing cellular damage from ischemia. In our study, in which iron deposition was noted on long TR/TE MR images shortly after clinical infarction, the iron accumulation may have resulted from direct tissue injury by iron-mediated peroxidation of membrane lipids. Importantly, since iron itself appears to be directly involved in the institution of the tissue damage, the detection of iron species may be useful as a means of monitoring future therapies and in predicting outcome. In fact, the extent of damage may be more accurately depicted by the iron pattern, a possibility suggested by the finding of bilateral iron deposition in all of our patients under 6 months of age who had any intracerebral iron, even those with unilateral infarctions.

A third situation in which hypointensity on MR images has been demonstrated in association with brain pathology is that of Wallerian degeneration. This phenomenon involves a nonspecific response to a variety of cerebral insults, most commonly infarction, whereby anterograde degeneration of the axonal projections follows axonal damage, leaving neuronal perikarya intact [28]. Axonal debris and myelin fragments are subsequently seen in phagocytic cells. The MR appearance of Wallerian degeneration has been shown both in animals [29] and humans [30]. In our cases, the rapid development of brain iron soon after infarction in some cases and its persistence for many months after infarction seem to exclude this explanation for the MR changes, since it has been shown that the hypointensity associated with Wallerian degeneration is transient and occurs approximately 4–12 weeks after clinical symptoms [30]. Additionally, the expected anatomic distribution of Wallerian degeneration-associated changes (e.g., along specific tracts) does not correlate with the sites of iron deposition seen in our cases.

Still another possible antecedent for basal ganglionic changes after cerebral infarction, especially in this age group, might include a disorder known as status marmoratus. This poorly understood entity derives its name from the streaked, marblelike appearance of the basal ganglia on gross pathology that was first described in patients with extrapyramidal disorders [31, 32], but also seen in infants after anoxic brain injury [33]. On microscopic examination, these regions consist of focal zones of gliosis with either increased or disorganized myelination patterns [33, 34]. In our study, the MR findings we observed were not those expected from such pathologic changes for at least three reasons: (1) selective hypointensity on long TR/TE images, as in our cases, would be consistent with iron, but *not* with signal intensity alterations seen in gliosis [35, 36]; (2) the intensity pattern in our cases on short TR/TE and long TR/TE images does not correspond to that of myelinated white matter; and (3) the marked increase in *degree* of hypointensity on gradient-echo images (in those cases in which these sequences were performed) indicated magnetic susceptibility-induced signal loss, a phenomenon caused by the presence of paramagnetic material, such as ferritin, rather than gliotic tissue and disorganized myelin.

In summary, although the mechanism of iron deposition in the brain is not fully understood, the MR appearance of increased iron seems to be a pathologic change that occurs in association with a variety of cerebral insults. We believe that the finding of iron deposition on MR is not at all specific to previously mentioned pathologic conditions with which iron has been documented to be associated (i.e., multiple sclerosis, Parkinson plus syndrome, and other movement disorders), but rather it should be regarded more in terms of being a final common pathway to axonal disruption. The ability of MR to detect in vivo a pathologically elevated intracerebral iron level may shed light on the role of iron in the pathophysiology of many ischemic and degenerative entities affecting the brain. While the true significance of this finding may merely be as an epiphenomenon—that is, as an indicator of brain injury that occurs as a concomitant of different pathologic processes—it remains to be seen whether the presence of abnormal intracerebral iron portends a different prognosis in these patients and whether this finding can be used as a tool for monitoring therapy.

REFERENCES

1. Gans A. Iron in the brain. *Brain* **1923**;46:128–136
2. Hallgren B, Sourander P. The effect of age on the non-haemin iron in the human brain. *J Neurochem* **1958**;3:41–51
3. Diezel PB. Iron in the brain: a chemical and histochemical examination. In: Waelsch H, ed. *Biochemistry of the developing nervous system.* New York: Academic Press, **1955**
4. Aoki S, Okada Y, Nishimura K, et al. Normal deposition of brain iron in childhood and adolescence: MR imaging at 1.5 T. *Radiology* **1989**;172: 381–385
5. Drayer B, Burger P, Hurwitz B, Dawson D, Cain J. Reduced signal intensity on MR images of thalamus and putamen in multiple sclerosis: increased iron content? *AJNR* **1987**;8:413–419
6. Drayer B, Olanow W, Burger P, Johnson GA, Herfkens R, Riederer S. Parkinson's plus syndrome: diagnosis using high field imaging of brain iron. *Radiology* **1986**;159:493–498
7. Rutledge JN, Hilal SK, Silver AJ, Defendini R, Fahn S. Study of movement disorders and brain iron by MR. *AJNR* **1987**;8:397–411
8. Craelius W, Migdal MW, Luessenhop CP, Sugar A, Mihalakis I. Iron deposits surrounding multiple sclerosis plaques. *Arch Pathol Lab Med* **1982**;106:397–399
9. Park BE, Netsky MB, Betsill WL. Pathogenesis of pigment and spheroid formation in Hallervorden-Spatz syndrome and related disorders. *Neurology* **1975**;25:1172–1178
10. Borit A, Rubenstein LJ, Urich H. The striatonigral degenerations: putaminal pigments and nosology. *Brain* **1975**;982:101–112

11. Earle KM. Studies on Parkinson's disease including X-ray fluorescent spectroscopy of formalin fixed brain tissue. *J Neuropathol Exp Neurol* **1968**;27:1–14
12. Hallgren B, Sourander P. The non-haemin iron in the cerebral cortex in Alzheimer's disease. *J Neurochem* **1960**;5:307–310
13. Dietrich RB, Bradley WG. Iron accumulation in the basal ganglia following severe ischemic-anoxic insults in children. *Radiology* **1988**;168:203–206
14. Gomori JM, Grossman RI, Goldberg HI, Zimmerman RA, Bilaniuk LT. Intracranial hematomas: imaging by high-field MR. *Radiology* **1985**; 157:87–93
15. Hecht-Leavitt C, Gomori JM, Grossman RI, et al. High field MR of hemorrhagic cortical infarction. *AJNR* **1986**;7:581–585
16. Harrison WW, Netsky M, Brown M. Trace elements in human brain: copper, zinc, iron and magnesium. *Clin Chim Acta* **1968**;21:55–60
17. Cummings JN. The copper and iron content of brain and liver in the normal and in hepatolenticular degeneration. *Brain* **1948**;71:410–415
18. Drayer B, Burger P, Darwin R, Riederer S, Herfkens R, Johnson GA. Magnetic resonance imaging of brain iron. *AJNR* **1986**;7:373–380, *AJR* **1986**;147:103–110
19. Gomori JM, Grossman RI, Yu-Ip C, Asakura T. NMR relaxation times of blood: dependence on field strength, oxidation state, and cell integrity. *J Comput Assist Tomogr* **1987**;11:684–690
20. Kim R, Ramachandran T, Parisi J, Collins G. Pallidonigral pigmentation and spheroid formation with multiple striatal lacunar infarcts. *Neurology* **1981**;31:774–777
21. Hill JM, Ruff MR, Weber RJ, Pert CB. Transferrin receptors in rat brain: neuropeptide-like pattern and relationship to iron distribution. *Proc Natl Acad Sci USA* **1985**;82:4553–4557
22. Jeffries WA, Brandon MR, Hunt SV, Williams AF, Gatter KC, Mason DY. Transferrin receptor density on endothelium of brain capillaries. *Nature* **1984**;312:162–163
23. Hill JM, Switzer RC. The regional distribution and cellular localization of iron in the rat brain. *Neuroscience* **1984**;11:595–603
24. Fahn S. Regional distribution studies of GABA and other putative neurotransmitters and their enzymes. In: Roberts E, Chase TN, Tower DB, eds. *GABA and nervous system function*. New York: Raven Press, **1976**: 169–186
25. White B, Aust S, Arfors K, Aronson L. Brain injury by ischemic anoxia: hypothesis extension—a tale of two ions. *Ann Emerg Med* **1984**;13: 862–867
26. Babbs C. Role of iron ions in the genesis of reperfusion injury following successful cardiopulmonary resuscitation: preliminary data and a biochemical hypothesis. *Ann Emerg Med* **1985**;14:777–783
27. Komara J, Nayini N, Bialick H, et al. Brain iron delocalization and lipid peroxidation following cardiac arrest. *Ann Emerg Med* **1986**;15:384–389
28. Adams JH, Corsellis JAN, Duchen LW, eds. *Greenfield's neuropathology,* 4th ed. New York: Wiley-Medical Publications, **1984**:15–17
29. Rafto SE, Wallace SF, Grossman RI, Rosenquist AC, Kundel HL. Magnetic resonance imaging in an animal model of Wallerian degeneration. Presented at the annual meeting of the American Society of Neuroradiology, Chicago, May **1988**
30. Kuhn MJ, Mikulis DJ, Ayoub DM, et al. Evolution of Wallerian degeneration following cerebral infarction: evaluation with sequential MR imaging. Presented at the annual meeting of the Radiological Society of North America, Chicago, November **1988**
31. Anton G. Über die betheiligung der basalen gehirnganglien bei bewegungsstörungen und insbesondere bei der chorea; mit demonstrationen von gehirnschnitten. *Wien Klin Wochenschr* **1893**;6:859–861
32. Oppenheim H, Vogt C. Nature et localisation de la paralyse pseudobulbaire congénitale et infantile. *J Psychol Neuro (Lpz)* **1911**;18:293–308
33. Friede RL, Schachenmayr W. EArly stages of staus marmoratus. *Acta Neuropathol (Berl)* **1977**;38:123–127
34. Borit A, Herndon RM. The fine structure of plaques fibromyéliniques in ulegyria and in status marmoratus. *Acta Neuropathol (Berl)* **1970**;14: 304–311
35. Braffman BH, Zimmerman RA, Trojanowski JQ, Gonatas NK, Hickey WF, Schlaepfer WW. Brain MR: pathologic correlation with gross and histopathology. 2. Hyperintense white-matter foci in the elderly. *AJNR* **1988**;9: 629–636, *AJR* **1988**;151:559–566
36. Marshall VG, Bradley WG Jr, Marshall CE, Bhoopat T, Rhodes RH. Deep white matter infarction: correlation of MR imaging with histopathologic findings. *Radiology* **1988**;167:517–522